ION BEAM ACCELERATION IN SYSTEM FROM PERIODIC SEQUENCE OF INDEPENDETLY PHASED CAVITIES

E.S. Masunov, A.V. Samoshin
Moscow Engineering Physics Institute (State University), Moscow, 115409, Russia
E-mail: ESMasunov@mephi.ru

Ion superconducting linac is based on periodic system consisting of the identical niobium cavities. By specific phasing of the RF cavities one can provide a stable particle motion in the whole accelerator. In this paper the beam stability conditions are founded. The matrix calculation and motion equation in the smooth approximation are used for alternating phase focusing analysis in superconducting linac.

PACS: 29.27.-A, 29.27.Bd

1. INTRODUCTION

Ion superconducting linac is usually based on the superconducting (SC) interdigital cavities. This linac consists of the niobium cavities which can provide typically 1 MV of accelerating potential per cavity. Such structures can be used for ion acceleration with different mass-charge ratio in the low energy region [1] and for proton linac in the high-energy region (SNS, JHF, ESS project). It is desirable to have a constant geometry of the accelerating cavity in order to simplify manufacturing. Such geometry leads to a non-synchronism but a stable longitudinal particle motion can be provided by proper phasing of the RF cavities. The ions are accelerated and slipping relative to the RF wave in dependence of the ratio between the particle velocity β and the phase velocity of the wave β_G. The geometrical velocity β_G of the RF wave is constant for cavities. The geometric size of a cavity and a wave velocity β_G must be changed step by step from one class to other class. The optimum number of cavity in each class determines the number of classes in SC linac. The identical cavities operate at the some initial drive phase φ. By controlling the driven phase of the accelerating structure and the distance between the cavities, the beam can be both longitudinally stable and accelerated in the whole system. In this paper two methods of the beam dynamics investigation are compared for low ion velocities and for the charge-to-mass ratio $Z/A = 1/66$. This comparison can be demonstrated with an example a post-accelerator of radioactive ion beams (RIB) linac, where beam velocity increases from $\beta = 0.01$ to $\beta = 0.06$ [1].

Beam focusing can be provided with help of SC solenoid lenses, following each cavity and with help of special RF fields. A schematic plot of one period of the accelerator structure is shown in Fig.1. The low-charge-state beams and the low velocity require stronger transverse focusing than one is used in existing SC ion linac. The large radial variation of the axial accelerating field induces a beam energy spread, which will accumulate as the beam passes through successive resonators. Early investigation of beam dynamics shown that for the initial normalized transverse emittance $\varepsilon_T = 0.1\pi$·mm·mrad and the longitudinal emittance $\varepsilon_V = 0.3\pi$·keV/u·nsec the connection between the longitudinal and transverse motion can be neglected if maximum beam envelop X_m < 3-4 mm and inner radius of accelerating drift tubes a = 15 mm.

2. BEAM STABILITY ANALISYS BY TRANSFER MATRICES

The general axisymmetric equations of motion for ion moving inside an accelerator can be written as

$$\begin{aligned}\frac{\mathrm{d}}{\mathrm{d}t}\left(m\gamma\frac{\mathrm{d}z}{\mathrm{d}t}\right) &= qE_z(\vec{r},t) - \frac{q^2}{2m\gamma}\frac{\partial}{\partial z}A_\varphi^2,\\ \frac{\mathrm{d}}{\mathrm{d}t}\left(m\gamma\frac{\mathrm{d}r}{\mathrm{d}t}\right) &= qE_r(\vec{r},t)\left(1-\beta\beta_G\right) - \frac{q^2}{2m\gamma}\frac{\partial}{\partial r}A_\varphi^2.\end{aligned} \quad (1)$$

In every cavity the acceleration RF field of periodic H-cavity is represented as an expansion in spatial harmonics

$$\left.\begin{aligned}E_z &= E_0\sum \mathrm{I}_0(h_n r)\cos\left(h_n(z-z_i)\right)\cos(\omega t)\\ E_r &= E_0\sum \mathrm{I}_1(h_n r)\sin\left(h_n(z-z_i)\right)\cos(\omega t)\end{aligned}\right\}, \quad (2)$$

where E_0 is amplitude of RF field at the axis ($E_0 \neq 0$ if $-L_r/2 < z-z_i < L_r/2$), $h_n = \pi/D + 2\pi n/D$, $n = 0, 1, 2, \ldots$, D is the period length of the cavity, L_r is the cavity length, z_i is the coordinate of the i-th cavity center. I_0, I_1 are modified Bessel function. In our case the reference particle velocity β_c and the geometrical velocity β_G are closely in each class of the identical cavities. Retaining in (2) only zeroth harmonic we can use the traveling wave system. In this system ωt can be replaced by $h_0(z-z_i) + \varphi_{0i}$, where φ_{0i} is the RF phase when the reference particle traverses the cavity center. In equation (1) the value A_φ is the azimuthal vector-potential of the magnetic field in every solenoid ($\boldsymbol{B} = \mathrm{rot}\boldsymbol{A}$).

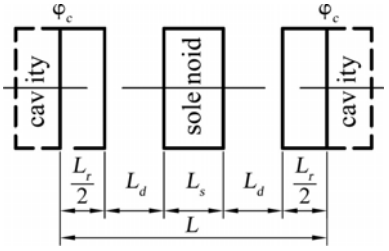

Fig.1. Layout of structure period

2.1. SOLENOID FOCUSING

From the motion equations (1) it can find the cavity, solenoid and drift space matrices M_{res}, M_{sol} and M_{dr}, if RF field and magnetic field amplitudes are approximated by the step function [2]. The transfer matrix for one period, M_z and M_r, are obtained by multiplying these matrices. The transfer matrices M_z and M_r allow to find the phase advances per period:

$$\mu_z = \arccos\left(\frac{1}{2}\left(M_{z11} + M_{z22}\right)\right), \qquad (3)$$

$$\mu_r = \arccos\left(\frac{1}{2}\left(M_{r11} + M_{r22}\right)\right). \qquad (4)$$

The longitudinal and transverse beam dynamics are stable if

$$\left|\cos\mu_z\right| \le 1, \left|\cos\mu_r\right| \le 1. \qquad (5)$$

From these inequalities it can compute the necessary magnetic field value B for a considered interval of beam velocity $0.01 \le \beta \le 0.06$. The choice of μ_z and μ_r is limited by the bunch size. In our case, the solenoid magnetic field B determines μ_r, the beta function and the extreme values of the beam envelope. For a charge-to-mass ratio $Z/A = 1/66$ and beam velocity range $0.01 < \beta_c < 0.02$ a proper focusing can be reached with magnetic fields up to 15 T, if $\mu_r < 25^0$. For beam velocities between 0.05 − 0.06c, the solenoid magnetic field B must be increased to obtain $\mu_r \approx 25^0$.

The final choice of the focusing magnetic field and the parameter μ_r can be made if the normalized transverse emittance V_r and maximum size of beam envelope X_m are fixed. In our case

$$\mu_r = \arcsin\left(\frac{V_r M_{r12}}{\beta\gamma X_m^2}\right), \qquad (6)$$

where M_{r12} is non-diagonal element of the transfer matrix. We can find the value of the focusing magnetic field $B_{\min}$ as function of the ion velocity β if the envelop X_m is the constant along the linac. The system of two equations (4) and (6) can be solved for X_m = const in the accelerator structure which consists of the periodic sequence of the solenoids and the resonators. For the acceleration phase φ_c=−20°, when the beam velocity increases from 0.01 to 0.06, the functions $B_{min}(\beta)$ decreases from 16 T to 10.5 T if the beam envelop X_m = 3 mm and from 14 T to 8 T if X_m = 4 mm.

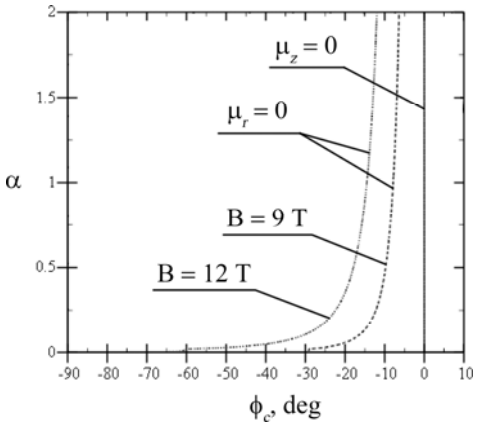

Fig.2. The beam stability area for different values of B

It is interesting to investigate the common stability area for longitudinal and transverse dynamics on the plane of variables α and φ, where the interaction parameter $\alpha = L\bar{U}/4L_v$, $\bar{U} = qU/m_ic^2$ is a dimensionless amplitude of accelerating potential per cavity, $m_i = Am_p$, $L_v = \lambda\beta^3\gamma^3/2\pi$, $L = L_{res} + 2L_d + L_{sol}$ is a period length, φ_c is reference particle phase. The borders of stability area between $\mu_z = 0$ and $\mu_r = 0$ are shown in Fig.2 for different values of magnetic field B, when $L_r/L = 1/4$. In our case the longitudinal dynamics is stable only if $\varphi_c < 0$. For $B = 0$ and $\varphi_c < 0$ the radial dynamics is instability. In this case the common area of beam stability is absent. This area appears and extends when magnetic field B increases. The minimum value of focusing field B_{min} can be founded from the condition $\mu_r = 0$. It's value depends on α and φ_c. When the beam velocity β_c increases the value of interaction parameter α (defocusing factor) quickly decreases ($\alpha \sim 1/\beta_c^3$). In this case the magnetic field B can be smaller for the same φ_c.

2.2. APF AND SOLENOID FOCUSING

The RF defocusing factor and required solenoid field are very large in the SC resonators. Another method of RF focusing is the alternating phase focusing (APF) [3]. Using transfer matrix calculations, we can study an alternating phase focusing structure in the superconducting linac by changing the sign of the reference phase value at each cavity [2]. Let's consider a simple case of the focusing period containing two SC cavities. By adjusting the phases φ_1 and φ_2 of each cavity individually, we can provide both acceleration and focusing. The phase advances per period, μ_z and μ_r, can be found from two transfer matrices M_z and M_r.

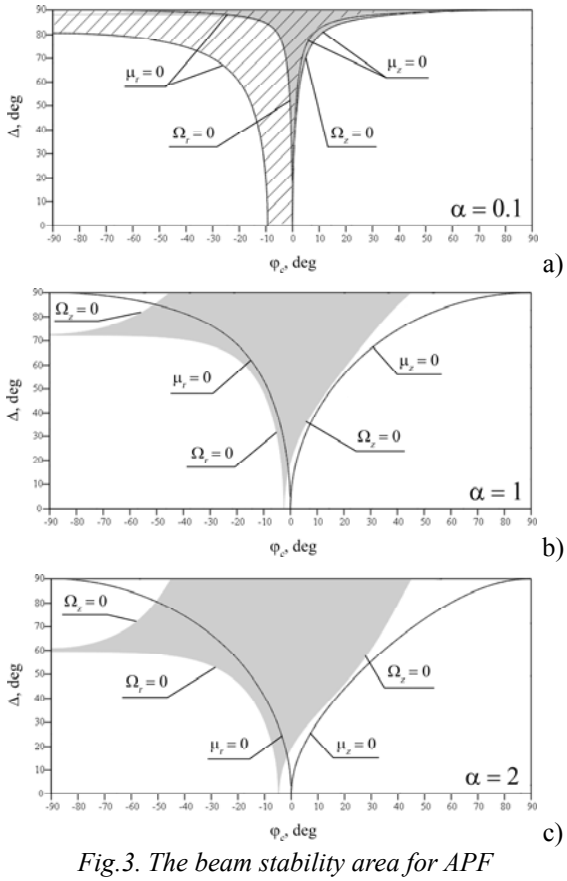

Fig.3. The beam stability area for APF

The borders of common stability area between $\mu_z = 0$ and $\mu_r = 0$ are shown in Fig.3 by black lines for deferent values of α, when $L_r/L = 1/4$. In this figure the new notations φ_c and Δ are used instead of $\varphi_{1,2} = \varphi_c \pm \Delta$. For the charge-to-mass ratio $Z/A = 1/66$ the parameter $\alpha \approx 1$, when the beam velocity $0.01 < \beta_c < 0.02$. In this case a large area of the stability on a plane (φ_c,Δ) is available. If the beam velocity $\beta_c > 0.03$, the parameter α becomes less than 0.1. For small α, the area of stability tapers

abruptly and the phase advances per period, μ_z and μ_r, quickly decrease. In this case the working point is located near stability borders.

The area of stability can be extended by adding a solenoid focusing which will also provide a separate control of transverse and longitudinal beam dynamics. For accelerator with SC solenoids this method was developed and studied both analytically [2] and with the help of the three-dimensional code TRACK [4]. It was shown that a combined focusing structure with solenoid and APF has obvious advantages compared to the reference design and can significantly reduce the cost of the linac. In our case for a beam velocity range of $0.03 < \beta_c < 0.04$ when $\alpha = 0.1$ it is sufficient to add one SC solenoid per accelerating period. If one solenoid with magnetic field B = 9 T is added, there is a large area of stability and a wide range of Δ and φ_c is possible. The stability diagram for $B = 9$ T is shown in Fig.3,a by the hatching.

3. BEAM STABILITY ANALISYS BY SMOOTH APPROXIMATION

In SC linac design, it is very important to know the bucket size since it relates to the longitudinal RF focusing. In this case the longitudinal acceptance cannot be obtained by matrix method because of the assumption that the particles have small longitudinal oscillation amplitude. In order to investigate the nonlinear ion beam dynamics in such accelerated structure and to calculate the longitudinal and transverse acceptances it can be used smooth approximation [5,6]. In periodical structure, which was shown in Fig.1, RF field can be expanded into a Fourier series as

$$E_z = \frac{U}{L}\mathrm{I}_0(k_0 r)\left\{f_{z.0} + \sum_1^\infty f_{z,n}^c \cos k_n z + f_{z,n}^s \sin k_n z\right\}$$
$$E_r = \frac{U}{L}\mathrm{I}_1(k_0 r)\left\{f_{r.0} + \sum_1^\infty f_{r,n}^c \cos k_n z + f_{r,n}^s \sin k_n z\right\} \quad (7)$$

Here $f_{z,0} = S_0\cos(\varphi_c + \psi)$, $f_{r,0} = -S_0\sin(\varphi_c + \psi)$,
$f_{z,n}^c = (-1)^n T_n^+ \cos(\varphi_c + \psi)$, $f_{z,n}^s = (-1)^{n+1} T_n^- \sin(\varphi_c + \psi)$
$f_{r,n}^c = (-1)^{n+1} T_n^+ \sin(\varphi_c + \psi)$, $f_{r,n}^s = (-1)^n T_n^- \cos(\varphi_c + \psi)$
$T_n^\pm = S_n^+ \pm S_n^-$, $S_n^\pm = \sin(Y_n^\pm)/Y_n^\pm$, $Y_n^\pm = (k_c \pm k_n)L_r/2$.

In this expressions: $E = 2U/L_r$, U is the cavity voltage amplitude; $k_n = 2\pi n/L$, $n = 0, 1, 2, \ldots$; k_c is slipping factor, $k_c = (2\pi/\lambda)(1/\beta_c - 1/\beta_G)$. In the coefficients $f_n^{c,s}$ the phase relative to the reference particle ψ defined by $\psi = \omega(t - t_c)$, t_c is the flight time of the reference particle.

In the simple case the vector-potential of the magnetic field $A_\varphi = Br/2$ can be approximated by the step function at every solenoid. If L_s is effective solenoid length and L is a lattice period, the external solenoid magnetic field can be represented as an expansion into spatial harmonics too.

3.1. SOLENOID FOCUSING

Let us consider particle acceleration in the polyharmonic fields of the cavities and solenoids. In general, individual particle motion is complicated but can be represented as the sum of a slow smooth motion (ψ and $\rho = h_0 r$) and a fast oscillation ($\tilde{\psi}$ and $\tilde{\rho}$). The force driving the ion motion can be separated into two parts corresponding to the fast and slow motion. Following Ref. [6] one can apply averaging over the fast oscillations and obtain the phase and radial motion equations in smooth approximation.

$$\frac{d^2\psi}{d\xi^2} + 3\left[\frac{d}{d\xi}(\ln\beta\gamma)\right]\frac{d\psi}{d\xi} = -\frac{\partial\overline{U}_{eff}}{\partial\psi}$$
$$\frac{d^2\rho}{d\xi^2} + \left[\frac{d}{d\xi}(\ln\beta\gamma)\right]\frac{d\rho}{d\xi} = -\frac{\partial\overline{U}_{eff}}{\partial\rho}, \quad (8)$$

where $U_{eff} = U_0 + U_1 + U_2$ is effective potential function. We use the following designations:

$$U_0 = 4\alpha\left[\mathrm{I}_0(\rho)\sin(\varphi_c + \psi) - \psi\cos\varphi_c - \sin\varphi_c\right]S_0 + \frac{1}{2}b\frac{L_c}{L}\rho^2$$

$$U_1 = \alpha^2\sum_1^\infty\left[\frac{\mathrm{I}_0^2(\rho)}{(2\pi n)^2}\left(f_{z,n}^{c\,2} + f_{z,n}^{s\,2}\right) + \frac{\mathrm{I}_1^2(\rho)}{(2\pi n)^2}\left(f_{r,n}^{c\,2} + f_{r,n}^{s\,2}\right)\right], \quad (9)$$

$$U_2 = -4\alpha b\rho\mathrm{I}_1(\rho)\frac{L_s}{L}\sum\frac{f_{r,n}^c}{(2\pi n)^2}\frac{\sin X_n}{X_n} + b^2\sum\frac{1}{(2\pi n)^2}\left(\frac{\sin X_n}{X_n}\right)^2\rho^2$$

Here $b = (qBL/2mc\beta_c\gamma_c)^2$, $X_n = \pi n L_s/L$.

The effective potential U_{eff} provides the full description of the ion dynamics in the smooth one-particle approximation. In Ref. [7] the longitudinal smooth approximation with acceleration in SC linac was investigated by the numerical simulation. In our case the analysis of the effective potential (9) makes it possible to study the condition at which the radial and phase stability of the beam is achieved. We begin our analysis with expanding U_{eff} in the vicinity of its minimum ($\psi = 0$, $\rho = 0$):

$$U_{eff} = U_{eff}(0,0) + \frac{1}{2}\Omega_z^2\psi^2 + \frac{1}{2}\Omega_r^2\rho^2 + \ldots \quad (10)$$

The expansion coefficients here depend on the parameter of interaction α, the values of L_r/L, L_s/L and the slipping factor k_c. The radial and phase stability of the beam will be provided when $\Omega_z^2 > 0$, $\Omega_r^2 > 0$, where Ω_z, Ω_r are dimensionless frequencies of small longitudinal and transverse oscillations.

In the simplest case when the phase velocity β_G changes from cavity to cavity and $k_c = 0$

$$\Omega_z = 2\sqrt{\alpha\sin(-\varphi_c) - \chi\alpha^2\cos(2\varphi_c)}$$
$$\Omega_r = \sqrt{-2\alpha\sin(-\varphi_c) + \chi\alpha^2\left(1 + \cos^2(\varphi_c)\right) + b\frac{L_s}{L}} \quad (11)$$

Here the value of χ depends on the ratio of L_r/L. For some of L_r/L the value of χ is listed in Table 1.

Table 1

L_r/L	0	1/4	1/2	1
χ	1/3	3/16	1/12	0

In single wave approximation when $L_r/L = 1$ and fast oscillation terms are absent, the value of $\chi = 0$. In this case, the dimensionless frequencies Ω_z, Ω_r are close to the longitudinal and transverse phase advances per a cavity μ_z and μ_r which were founded by transfer matrix calculation. But the conditions of focusing are changed if the parameter α is large and the fast oscillations are

considered. The functions $\Omega_z(\alpha)$ and $\Omega_r(\alpha)$ for different values of φ_c are shown in Fig.4. The phase advances should be less than about $\pi/2$ for stable beam motion [8]. In this case, the smooth approximation is expected to be almost accurate and dimensionless frequencies Ω_z, Ω_r are close to the phase advances per a period μ_z and μ_r.

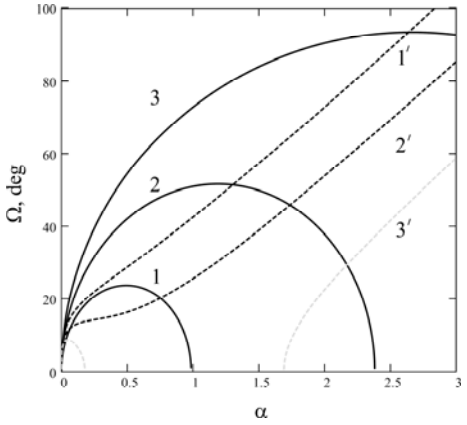

Fig.4. The frequencies of longitudinal (solid lines) and transverse (dot lines) oscillations for B = 12 T (1 – $\varphi_c = -10°$, 2 – $\varphi_c = -20°$ and 3 – $\varphi_c = -30°$)

As it can see from Fig.4, the longitudinal oscillation will be stability for $-\pi/4 < \varphi_c < 0$ if the interaction parameter α is limited, $\alpha < \alpha_{max} = \sin(-\varphi_c)/\chi\cos(2\varphi_c)$. In this case the frequency of longitudinal oscillation has maximum value in $\alpha = \alpha_{max}/2$. If the magnetic field is absent the radial stability of the beam is achieved, if the interaction parameter $\alpha > \alpha_{min} = 2\sin(-\varphi_c)/\chi(1+\cos^2\varphi_c)$

The borders of stability area between $\Omega_z = 0$ and $\Omega_r = 0$ are shown in Fig.5 for deferent values of magnetic field, B, when $L_r/L = 1/4$.

The value α on stability diagram moves down quickly on the $\alpha = 0$ axis when the beam velocity increases. For $B = 0$, the area of stability exists but it tapers abruptly and the radial stability is absent when the beam velocity increases. The common area of stability can be extended by a solenoid focusing which will also provide a separate control of transverse and longitudinal beam dynamics. For beam velocity $\beta \geq 0.1$, $\alpha \approx 2$ it is sufficient to increase the solenoid field $B = 12$T if the reference particle phase $\varphi_c > -20°$.

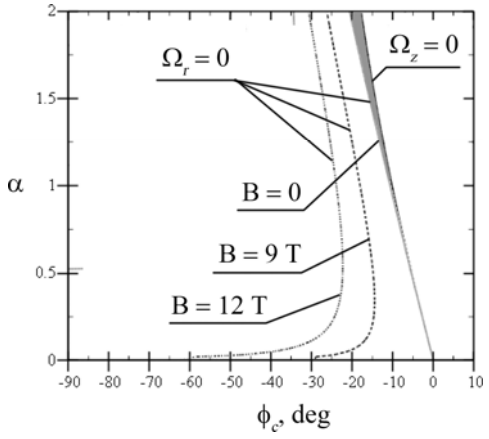

Fig.5. Stability area for different values of the magnetic field B

3.2. APF AND SOLENOID FOCUSING

The smooth approximation has been applied to the study of APF in RIB linac. New effective potential U_{eff} must be find for this accelerating structure. The analysis of the effective potential makes it possible to study the condition at which the radial and phase stability of the beam is achieved. In the simplest case when a slipping factor $k_c = 0$ it can find the dimensionless frequencies of the small oscillations:

$$\Omega_z^2 = -8\alpha\left\{\cos\Delta\sin\varphi_c + \right.$$
$$\left. +\alpha\left[\chi_1\cos^2\Delta - \chi_2\sin^2\Delta\right]\cos\left(2\varphi_c\right)\right\}, \quad (12)$$

$$\Omega_\rho^2 = 4\alpha\left\{\cos\Delta\sin\varphi_c + \right.$$
$$\left. +\frac{\alpha}{2}\left[\chi_1\cos^2\Delta\left(1+\cos^2\varphi_c\right)+\chi_2\sin^2\Delta\left(1+\sin^2\varphi_c\right)\right]\right\}. \quad (13)$$

In this expressions $\varphi_{1,2} = \varphi_c \pm \Delta$ are reference particle phases in the neighbour cavities, the values of $\chi_{1,2}$ depend on the ratio of L_r/L (see Table 2). The common area of the beam stability is shown in Fig.3 by the filling. This area is located between the borders where $\Omega_z = 0$ and $\Omega_r = 0$.

Table 2

L_{res}	0	$L/4$	$L/2$	L
χ_1	1/6	1/24	0	0
χ_2	1/2	1/3	1/6	0

The analysis of APF for the charge-to-mass ratio $Z/A = 1/66$ shows that the effective focusing and acceleration are realized, when the beam velocity $0.01 < \beta_c < 0.02$ and the cavity length is small ($L_r/L < 1/4$). The longitudinal and transverse stabilities are realized simultaneously only for a small asymmetry at the choice of the reference particle phases ($\varphi_c = -5°$) and for large value Δ. If the value of Δ increases the rate of energy gain reduces. The working point is located near right side of beam stability border where $\Omega_z = 0$ for symmetric choice of the reference particle phases ($\varphi_c = 0$). In this case the longitudinal acceptance is very small.

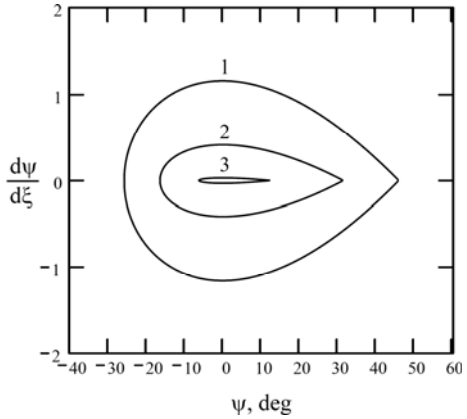

Fig.6. Separatrixes for $\varphi_c = -5°$, $\Delta = 45°$ and $\rho = 0$ for different parameter α: 1 – $\alpha = 2$, 2 – $\alpha = 1$ and 3 – $\alpha = 0.1$

It is interesting to investigate the nonlinear ion beam dynamics in such accelerated structure. Using of the

effective potential U_{eff} we can calculate the longitudinal acceptance. In Fig.6 it is shown the separatrixes for $\varphi_c = -5°$, $\Delta = 45°$ and $\rho = 0$ when the beam velocity increases and the parameter α decreases from 2 to 0.1. The energy spread of the separatrix, $\Delta\gamma = (L_1/L)(d\psi/d\xi)$, decreases in 10 times and the phase length Ψ of separatrix decreases in 3 times. In this case longitudinal acceptance decreases in 15 times. If the value of the cavity voltage amplitude U is preset the separatrix area depends on the value of L_r/L ratio. The smooth approximation gives a weaker effective RF bucket, i.e. smaller phase acceptance and potential well depth, compared with the single wave approximation when the fast oscillations are not considered.

For small α the value of longitudinal acceptance quickly decreases and size of beam envelope X_m increases. These disadvantages of APF can be removed by adding a focusing solenoid into focusing period which will also allow separate control of the transverse and longitudinal beam dynamics. The combination of low-field SC solenoids and APF is very effectively at all range of beam velocity $0.02 \le \beta \le 0.06$. The combined focusing structure includes both SC solenoid and APF in every focusing period. The transverse focusing can be realized in the magnetic field $B \le 6$ T for maximum value of beam envelop X_m=4 mm and $B \le 9$ T for beam envelop X_m=3 mm. But in this case the longitudinal focusing will become worse because the longitudinal oscillation frequency Ω_z will be small.

CONCLUSION

Two methods of the focusing analysis are compared for low ion velocities. The low charge state beams require stronger transverse focusing in RIB linac. In order to reduce the cost of the SC solenoids it can be used APF or the combination of low-field SC solenoids and ARF. By the smooth approximation it is studied more detailed nonlinear ion beam dynamics and found the borders of the beam stability area. It is done the recommendation for choice of the reference particle phases and the value of solenoid magnetic field B.

REFERENCES

1. P.N. Ostroumov, et al. // *Proc. of PAC2001*. Chicago, IL, June 18-21, 2001, p.4080.
2. E.S. Masunov, P.N. Ostroumov, et al. // *Proc. of PAC2003*. Portland, June 2001, p.2963.
3. Y.B. Faynberg // *Zh. Tekn. Fiz.* 1959, v.29, p.568.
4. P.N. Ostroumov, E.S. Masunov, et al. // *Proc. of the LINAC'2004*. Lubeck, Germany, p.348.
5. P.L. Kapitsa, *Zh. Eksp. Teor. Fiz.* 1951, v.21, p.588.
6. E.S. Masunov, N.E. Vinogradov // *Phys. Rev. ST-AB*. 2001, v.4, 070101.
7. Ji Qiang, R.W. Garnett // *Nucl. Instr. and Meth.* 2003, v.A496, p.33.
8. L.J. Hofmann. Laslett, et al. // *Part. Acc.* 1983, v.13, p.145.

УСКОРЕНИЕ ИОННОГО ПУЧКА В СИСТЕМЕ ИЗ ПЕРИОДИЧЕСКОЙ ПОСЛЕДОВАТЕЛЬНОСТИ НЕЗАВИСИМО ФАЗИРУЕМЫХ РЕЗОНАТОРОВ

Э.С. Масунов, А.В. Самошин

Сверхпроводящий линейный ускоритель ионов основан на использовании периодической системы, состоящей из идентичных ниобиевых резонаторов. Посредством специального фазирования ВЧ-резонаторов можно обеспечить устойчивое движение частиц во всем ускорителе. В этой статье найдены условия устойчивости движения пучка ионов. Матричный метод расчета и уравнение движения в гладком приближении используются для анализа фазопеременной фокусировки пучка в сверхпроводящем ускорителе.

ПРИСКОРЕННЯ ІОННОГО ПУЧКУ У СИСТЕМІ З ПЕРІОДИЧНОЮ ПОСЛІДОВНІСТЮ НЕЗАЛЕЖНО ФАЗУЄМИХ РЕЗОНАТОРІВ

Е.С. Масунов, А.В. Самошин

Надпровідний лінійний прискорювач іонів заснований на використанні періодичної системи, що складається з ідентичних ніобієвих резонаторів. За допомогою спеціального фазування ВЧ-резонаторів можна забезпечити стійкий рух часток у всьому прискорювачі. У статті знайдено умови стійкості руху пучка іонів. Для аналізу фазозмінного фокусування пучка у надпровідному прискорювачі використано матричний метод розрахунку і рівняння руху у гладкому наближенні.